Tuning the Negative Photochromism of Water

Soluble Spiropyran Polymers

Matthew J. Feeney and Samuel W. Thomas III\*

Department of Chemistry, 62 Talbot Avenue, Tufts University, Medford, MA 02155

ABSTRACT: In aqueous media, negative photochromism can occur from cationic, protonated merocyanines (MCH<sup>+</sup>) to spiropyrans (SP) upon exposure to visible light. Herein, we demonstrate the uniquely simple manner in which polymers can tune the key properties of these photochromes through copolymer preparation. Nine water-soluble, SP-containing polymers yield wide ranges of key properties for negative photochromism—accessible MCH<sup>+</sup> pKa values spanning 5 pH units, quantum yields of photochemical ring closure up to 0.2, and rates of thermal equilibration ranging two orders of magnitude. In buffered solutions, many of these polymers showed photostationary states with greater than 80% conversion to SP and no detectable photochromic fatigue over fifteen cycles. These results demonstrate the potential for tuning key properties of the MCH+ photochrome through both the spiropyran pendants themselves and the water-solubilizing comonomers. The dependence of MCH<sup>+</sup> pKa on comonomer structure enabled tunable range of pH for reversible photoacid activity using a single spiropyran derivative, further showcasing the versatility of water-soluble photochromic polymers.

#### Introduction

Stimuli-responsive materials are invaluable for the further development of tools in numerous areas of research, 12 including drug delivery platforms and sensors. 4 More specifically, reversibly responsive materials present unique opportunities for a range of applications, such as real-time imaging and logic gates. 6 Compared to other stimuli, light has a unique combination of advantages: enhanced spatial resolution, selectivity derived from wavelengths of light with readily tunable energies, and potential for permeability through barriers impervious to other reagents. 7 In addition to irreversible photochemical reactions, such as with photoremovable protection groups, 8 a number of light-driven processes allow for reversible transformations.

The two most common classes of reversible photoreactions are photo-dimerizations<sup>9</sup> (especially [2+2] and [4+4] cycloadditions) and photo-isomerizations.<sup>10</sup> Photochromes are molecules that undergo reversible photo-isomerizations that yield different colors of interchangeable isomers. A variety of photochromic moieties exist, and can be categorized into either: i) T-type photochromes, for which reversion to the more stable isomer can occur thermally (including azobenzenes and spiropyrans), and ii) P-type photochromes, for which interconversions in both directions require irradiation (such as dithienylethenes).<sup>11-13</sup> Upon irradiation with ultraviolet (UV) light, spiropyran (SP) derivatives undergo isomerization to metastable merocyanine (MC) isomers, which can thermally or photochemically revert to SP. While SP is an uncharged, hydrophobic molecule, the ring-open MC is a zwitterion with strongly delocalized electron density. The SP-to-MC conversion also yields a drastic coloration of the sample due to the highly conjugated and donor-acceptor nature of MC.

Much of the literature on spiropyran containing materials has focused on photochromism in hydrophobic and organic media, especially of 6-nitrospiropyran derivatives, which are efficient in both UV-induced MC formation and thermal or photochemical reversion.<sup>14</sup> Integration of SP photochromes into aqueous systems, which is important for biological applications, is comparatively rare.<sup>15,16</sup> A key difference in the behavior of spiropyrans in aqueous media is the increased importance of a third species: protonation of the MC phenoxide yields the cationic MCH<sup>+</sup>, which has an absorbance band between those of SP and MC.<sup>17,18</sup> Thus, three chemical species—SP, MC, and MCH<sup>+</sup>, each with unique physical and chemical properties—are potentially accessible, especially when spiropyran molecules are in protic media (*Figure 1*).

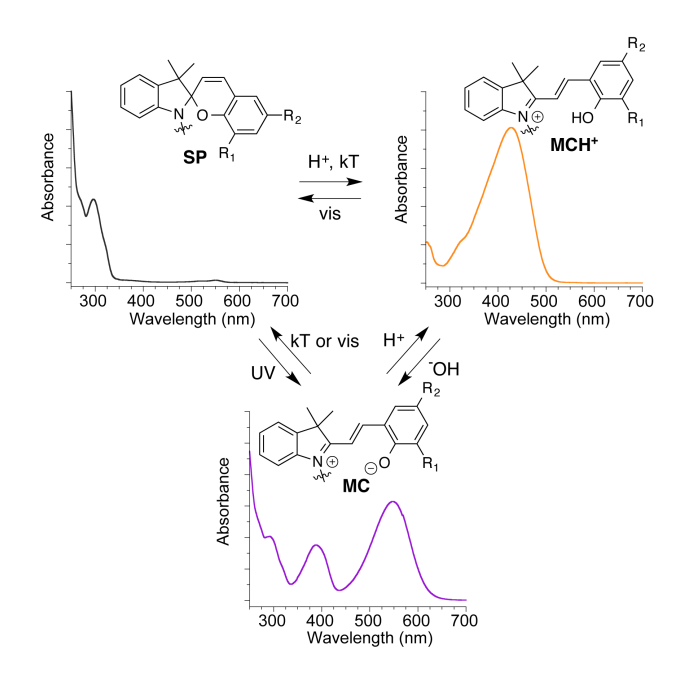


**Figure 1.** Reversible interconversions between SP (top, left), MCH<sup>+</sup> (top, right), and MC (bottom) species, as well as representative UV/vis absorbance spectra in water when attached as pendants to water soluble polymers (SP, MCH<sup>+</sup>: **HSp-PEGMA**. MC: **HSp-DMAEMA**)

The presence of the MCH<sup>+</sup> species in aqueous solution has important consequences. First, the equilibrium among species shifts dramatically. At pH values below the pKa of MCH<sup>+</sup> phenol, negative photochromism occurs with a transition from colored MCH<sup>+</sup> to uncolored SP upon

exposure to visible light.<sup>19,20</sup> Regeneration of the MCH<sup>+</sup> species occurs either by thermal equilibration or upon UV exposure. Second, reversible proton dissociation can occur in specific pH ranges upon isomerization, since MCH<sup>+</sup> is less acidic than the protonated ring-closed form (SPH<sup>+</sup>).<sup>19</sup> This reversible photoacidity has been demonstrated to change solution pH by over 2 orders of magnitude.<sup>21-26</sup> Light-controlled acidity has proven useful in pH-responsive functions, such as reversible patterning,<sup>25,27-29</sup> control over nanoparticle formation and aggregation,<sup>30-32</sup> supramolecular assembly and polymerization,<sup>33-36</sup> and targeting pH sensitive biological species.<sup>37,38</sup> Additional functions of the MCH<sup>+</sup> species that are not derived from changes in solution pH include self-assembly of amphiphilic structures<sup>39-41</sup> and sensing.<sup>42</sup>

Imparting water solubility to spiropyrans can be accomplished through incorporation of the photochromic moieties into water-soluble polymers such as acrylamides. <sup>19,43-45</sup> *N*-isopropylacrylamide (NIPAM) is an example of a water-solubilizing comonomer, which together with the photochromic reactions of spiropyran, can yield polymers that respond to multiple stimuli. <sup>43,46,47</sup> However, copolymerization with various ionic monomers to afford polyelectrolytes can also impart water solubility while also influencing polymer physical properties. For example, the electrostatic environment surrounding an acidic moiety can have a strong influence over acid strength. In weak polyacids, an increase in ionization leads to an increase in pKa of the nonionized sidechains, rationalized by an electrostatic cost associated with removal of a proton from a highly negatively charged species. <sup>48-52</sup> The opposite holds true for polybases, as increased positive charge due to ionization increases acidity. <sup>53</sup>

Additionally, modification of the spiropyran chromene ring with both electron withdrawing and electron donating substituents directly influences photochromic properties.<sup>54,55</sup> In organic media, 6-nitrospiropyran is both readily prepared and shows highly efficient photochromism, and

is therefore the most extensively utilized derivative. In aqueous solutions, the ranges of spiropyran structures that show efficient negative photochromism are broad; for example, Sumaru and coworkers reported a comparison of the isomerization kinetics of water soluble acrylamide-based polymers with unsubstituted, methoxy-, and nitro-spiropyran pendants.<sup>54</sup>

Herein we report a series of spiropyran-containing hydrophilic polymers, and elucidation of how their chemical structures influence MCH<sup>+</sup> acidity as well as efficiencies of negative photochromism in water. The structures of these polymers vary in two ways: i) the substituent effects of methoxy or nitro groups on the chromene unit of the spiropyran photochrome itself, and ii) the charge on photoinert, hydrophilic comonomers to both impart water solubility and present different electrostatic environments—cationic, neutral, or anionic—to the spiropyran/merocyanine photochrome. Variations of substituents on the SP pendants and comonomer structures yield diverse properties, with isomerization rates spanning two orders of magnitude, and acidities of MCH<sup>+</sup> spanning five pH units. Such broadly applicable relationships of the structures of photochromic polymers are important for the further development of photoresponsive materials in aqueous environments.

## **Experimental Section**

#### Materials

All synthetic steps utilized air-free techniques under argon atmosphere with magnetic stirring. Silica gel (230-400 mesh), neutral aluminum oxide, and basic aluminum oxide were used as stationary phases for flash chromatography. Commercial chemicals were used without further purification unless otherwise noted. Dry solvents were obtained from an Innovative

Technologies PureSolv 400 solvent purifier. Ethanol was distilled prior to use. Potassium ferrioxalate was recrystallized from water twice prior to use.

Characterization by NMR spectroscopy was performed on a Bruker Avance III 500 or Bruker DPX-300 spectrometer. Molecular weight distributions of polymers were determined with a Shimadzu gel permeation chromatograph (GPC) equipped with UV and refractive index detectors. For measurement of PEGMA and DMAEMA polymers, a Tosoh Bioscience TSKgel GMHHRM column (7.8 mm ID x 30 cm, 5 µm) equipped with a TSKgel Guard HHR-H (6 mm ID x 4.0 cm, 5 μm) was used with reference to polystyrene standards. For PEGMA polymers, tetrahydrofuran (THF) was used as the mobile phase, while for DMAEMA polymers, 2% triethylamine in THF was used as the mobile phase, with a flow rate of 0.75 mL/min for both systems. For measurement of AMPS polymers, Waters Ultrahydrogel 250 (7.8 x 300 mm) and Ultrahydrogel 120 (7.8 x 300 mm) columns were used in series, equipped with a Waters Ultrahydrogel guard column (6 x 40 mm). AMPS samples were eluted with a mobile phase of 0.1 M sodium nitrate (aq), with reference to poly(ethylene glycol) standards. Absorbance measurements of liquid samples were performed in quartz glass (NSG Precision Cells) or poly(methyl methacrylate) plastic (Fisher Scientific) cuvettes using a Varian Cary 100 spectrophotometer in double beam mode. Quartz cuvettes were utilized specifically for pKa and quantum yield measurements. Irradiations were performed with a 200 W Hg/Xe lamp (Newport-Oriel) equipped with a condensing lens and a recirculating water filter. Specific wavelengths of light were selected through the singular or combined use of multiple filters: 295 and 530 nm long-pass filters (Newport), and a 404 nm interference filter (Newport).

Scheme 1. Synthesis of spiropyran-containing statistical copolymers. Feed ratios of monomers were m:n 1:19.

## Chemical synthesis

Compounds 1-3 were synthesized according to a previously reported procedure.<sup>56</sup> Synthesis of monomers 4-7, and all polymers proceeded as follows.

## *HSpOH* (4)

To a solution of 1 (1.00 g, 3.52 mmol) in water (15 mL) was added potassium hydroxide (316 mg, 5.63 mmol). The reaction mixture was stirred for 15 minutes at room temperature, extracted with diethyl ether three times, dried over MgSO<sub>4</sub>, and concentrated. The resulting brown oil was dried *in vacuo* and carried forward without purification. To a solution of the oil (626 mg, 3.08 mmol) in ethanol (15 mL) was added salicylaldehyde (0.34 mL, 3.23 mmol). The reaction was heated to reflux overnight. After 16 h, the reaction mixture was concentrated, and precipitated from EtOH into H<sub>2</sub>O twice, affording 4 as a brown foam (797 mg, 74%), which was carried onto the next step without further purification. <sup>1</sup>H NMR (500 MHz, CDCl<sub>3</sub>): δ (ppm) 7.16 (t, 1H), 7.11-7.03 (m, 2H), 6.87-6.82 (m, 3H), 6.70 (d, 1H), 6.64 (d, 1H), 5.67 (d, 1H), 3.79-3.70 (m,

2H), 3.55-3.50 (m, 1H), 3.37-3.32 (m, 1H), 1.91 (t, 1H), 1.30 (s, 3H), 1.18 (s, 3H). <sup>13</sup>C NMR (125 MHz, CDCl<sub>3</sub>): δ (ppm) 153.9, 147.4, 136.5, 129.9, 129.5, 127.6, 126.9, 121.9, 120.5, 119.6, 119.3, 118.6, 115.1, 106.6, 104.6, 60.9, 52.3, 46.1, 25.9, 20.4.

## *HSpMA* (5)

To a solution of **4** (664 mg, 2.16 mmol) in dichloromethane (10 mL) was added triethylamine (0.45 mL, 3.2 mmol). To the reaction mixture at 0 °C was added methacryloyl chloride (0.32 mL, 3.2 mmol). The reaction was allowed to warm to 25 °C and stirred overnight. After 16 h, the reaction was diluted with dichloromethane, washed with 0.1 M NaHCO<sub>3</sub> once, saturated NaCl (aq) twice, dried over MgSO<sub>4</sub>, and concentrated. The residue was concentrated onto Celite and purified by silica gel flash chromatography (5-10% ethyl acetate/hexanes) to afford **5** as a colorless oil (330 mg, 41%). <sup>1</sup>H NMR (300 MHz, CDCl<sub>3</sub>): δ (ppm) 7.18 (t, 1H), 7.12-7.03 (m, 3H), 6.89-6.80 (m, 3H), 6.69 (d, 2H), 6.09 (s, 1H), 5.69 (d, 1H), 5.56 (s, 1H), 4.30 (t, 2H), 3.66-3.56 (m, 1H), 3.45-3.36 (m, 1H), 1.93 (s, 3H), 1.30 (s, 3H), 1.15 (s, 3H). <sup>13</sup>C NMR (75 MHz, CDCl<sub>3</sub>): δ (ppm) 167.3, 154.1, 147.2, 136.4, 136.2, 129.8, 129.5, 127.6, 126.8, 125.7, 121.7, 120.2, 119.5, 119.2, 118.5, 115.1, 106.5, 104.5, 63.02, 52.2, 42.4, 25.9, 20.1, 18.4.

# *OMeSpOH* **(6)**

To a solution of **1** (2.00 g, 7.04 mmol) in water (28 mL) was added potassium hydroxide (632 mg, 11.3 mmol). The reaction mixture was stirred for 15 minutes at room temperature, extracted with diethyl ether four times, dried over MgSO<sub>4</sub>, and concentrated. The resulting brown oil was dried *in vacuo* and carried forward without purification. To a solution of the oil (1.32 g, 6.51 mmol) in ethanol (30 mL) was added *o*-vanillin (1.04 g, 6.83 mmol). The reaction was heated to reflux overnight. After 16 h, the reaction mixture was concentrated, dissolved in dichloromethane, washed with 0.1 M NaOH once, deionized water once, sat NaCl (aq) once, and

then dried over MgSO<sub>4</sub> and concentrated. The sample was recrystallized from CH<sub>2</sub>Cl<sub>2</sub>/hexanes, affording **6** as a green solid (1.32 g, 56%), which was carried forward without further purification. <sup>1</sup>H NMR (500 MHz, CDCl<sub>3</sub>): δ (ppm) 7.14 (t, 1H), 7.06 (d, 1H), 6.83-6.74 (m, 4H), 6.67 (d, 1H), 6.61 (d, 1H), 5.63 (d, 1H), 3.83-3.77 (m, 1H), 3.70-3.58 (m, 5H), 3.42-3.37 (m, 1H), 2.35 (t, 1H), 1.31 (s, 3H), 1.16 (s, 3H). <sup>13</sup>C NMR (125 MHz, CDCl<sub>3</sub>): δ (ppm) 147.3, 147.1, 142.9, 136.2, 129.3, 127.4, 121.9, 120.1, 120.1, 119.4, 119.1, 118.9, 113.4, 106.4, 104.3, 60.5, 56.2, 52.4, 45.8, 25.9, 20.5.

## OMeSpMA (7)

To alcohol **6** (1.00 g, 2.96 mmol) was added dichloromethane (30 mL), and triethylamine (0.62 mL, 4.4 mmol). To the reaction mixture at 0 °C was added methacryloyl chloride, and the reaction was allowed to warm to 25 °C and stir overnight. After 16 h, the reaction was diluted with CH<sub>2</sub>Cl<sub>2</sub>, and washed with 0.1 M NaOH once, deionized water once, saturated NaCl (aq) once, dried over MgSO<sub>4</sub>, and concentrated. The residue was concentrated onto Celite and purified by flash chromatography on neutral alumina (3-9% ethyl acetate/hexanes). The collected sample was further purified by recrystallization from hexanes, affording **7** as a yellow solid (166 mg, 14%).

<sup>1</sup>H NMR (300 MHz, CDCl<sub>3</sub>): δ (ppm) 7.15 (t, 1H), 7.06 (d, 1H), 6.86-6.65 (m, 6 H), 6.08 (s, 1H), 5.69 (d, 1H), 5.55 (s, 1H), 4.30 (t, 3H), 3.69-3.60 (m, 4H), 3.49-3.39 (m, 1H), 1.92 (s, 3H), 1.30 (s, 3H), 1.14 (s, 3H). <sup>13</sup>C NMR (125 MHz, CDCl<sub>3</sub>): δ (ppm) 167.3, 147.3, 147.2, 143.7, 136.4, 136.2, 129.3, 127.4, 125.6, 121.7, 120.0, 119.8, 119.4, 119.3, 119.0, 114.2, 106.4, 104.5, 63.0, 56.5, 52.2, 42.3, 25.9, 20.1, 18.4.

#### NO<sub>2</sub>Sp-PEGMA

Poly(ethylene glycol)methyl ether methacrylate (PEGMA) was eluted from a plug of basic alumina to remove inhibitor. To a Schlenk flask was added 3 (90 mg, 0.21 mmol) in anhydrous THF (5 mL), PEGMA (1.16 mL, 4.07 mmol), ethyl  $\alpha$ -bromoisobutyrate (EBiB, 12.6  $\mu$ L, 0.086 mmol), and copper (I) bromide (12.3 mg, 0.086 mmol). The mixture was degassed via three freeze-pump-thaw cycles. To the reaction mixture under argon added was pentamethyldiethylenetriamine (PMDETA, 35.7 µL, 0.171 mmol), which had been sparged previously with argon for 30 minutes. The reaction mixture was heated at 65 °C overnight. After 16 h, the reaction was removed from heat and exposed to air. The reaction was precipitated into hexanes, affording a green solid. The solid was dissolved THF, eluted through a plug of neutral aluminum oxide, and concentrated. The residue was dissolved in chloroform and precipitated into hexanes, affording NO<sub>2</sub>Sp-PEGMA as a viscous maroon gel. (503 mg, 38%. M<sub>n</sub>: 32 kDa,  $M_w$ : 52 kDa) <sup>1</sup>H NMR (500 MHz, CDCl<sub>3</sub>):  $\delta$  (ppm, broad signals) 8.06-8.02, 7.23-6.65, 5.97-5.86, 4.15-4.00, 3.71-3.58, 3.57-3.52, 2.10-0.70. (2.10-1.59, 1.53-1.13, 1.10-0.70).

## NO<sub>2</sub>Sp-DMAEMA

To a solution of **3** (85 mg, 0.20 mmol) in toluene (6.8 mL) was added azobisisobutyronitrile (AIBN, 6.8 mg), and *N*,*N*-dimethylaminoethyl methacrylate (DMAEMA, 0.65 mL, 3.8 mmol). The reaction mixture was deoxygenated via sparging with argon for 25 min, and then heated at 65 °C overnight. After 2 days, the reaction was cooled and precipitated from CHCl<sub>3</sub> into hexanes twice, affording **NO**<sub>2</sub>**Sp-DMAEMA** as a red solid. (460 mg, 67%. M<sub>n</sub>: 14 kDa, M<sub>w</sub>: 23 kDa) <sup>1</sup>H NMR (500 MHz, CDCl<sub>3</sub>): δ (ppm) 7.24-6.64, 5.96-5.82, 4.20-3.90, 3.55-3.34, 2.62-2.46, 2.45-2.39, 2.33-2.18, 2.17-2.13, 2.00-0.79.

#### NO<sub>2</sub>Sp-AMPS

To a solution of **3** (62 mg, 0.15 mmol) was added 2-acrylamido-2-methylpropane sulfonic acid (AMPS, 580 mg, 2.80 mmol), AIBN (6.5 mg), and DMF (6.5 mL). The reaction mixture was fully dissolved by stirring for 15 minutes, and then degassed via three freeze-pump-thaw cycles. The reaction was heated at 65 °C under argon overnight. After 16 h, the reaction was cooled, precipitated into ethyl acetate, dissolved in water, and dialyzed against water (MWCO 3.5 kDa) for 2 d. The aqueous solution was concentrated under vacuum and dried via azeotropic distillation with ethanol, affording **NO<sub>2</sub>Sp-AMPS** as a brown solid. (203 mg, 32%. M<sub>n</sub>: 7 kDa, M<sub>w</sub>: 9 kDa) <sup>1</sup>H NMR (500 MHz, D<sub>2</sub>O): δ (ppm) 8.95-7.54, 7.35-6.83, 4.24-4.04, 3.73-2.99, 2.37-0.66.

#### HSp-PEGMA

PEGMA was eluted from a basic alumina plug to remove inhibitor. To a Schlenk flask was added 5 (101 mg, 0.269 mmol) in anhydrous THF (6.3 mL), PEGMA (1.46 mL, 5.11 mmol), EBiB (15.8 μL, 0.108 mmol), and copper (I) bromide (15.5 mg, 0.108 mmol). The mixture was degassed via three freeze-pump-thaw cycles. To the reaction mixture under argon was added PMDETA (44.9 μL, 0.215 mmol), which had been previously sparged with argon for 30 minutes. The reaction mixture was heated at 65 °C overnight. After 16 h, the reaction was removed from heat and exposed to air. The reaction was diluted with CH<sub>2</sub>Cl<sub>2</sub>, filtered through a neutral aluminum oxide plug, concentrated, and precipitated out of chloroform into hexanes twice, affording **HSp-PEGMA** as a gel. (840 mg, 51%. M<sub>n</sub>: 26 kDa, M<sub>w</sub>: 40 kDa) <sup>1</sup>H NMR (300 MHz, CDCl<sub>3</sub>): δ (ppm) 7.20-7.00, 6.94-6.78, 6.74-6.61, 5.77-5.63, 4.32-4.28, 4.25-3.94, 3.92-3.83, 3.80-3.47, 3.45-3.27, 2.17-1.67, 1.56-0.65.

#### HSp-DMAEMA

To a solution of **5** (50 mg, 0.13 mmol) in toluene (4.5 mL) was added DMAEMA (0.43 mL, 2.5 mmol) and AIBN (4.5 mg). The reaction mixture was deoxygenated by sparging with argon for 25 min, and then heated at 65 °C overnight. After 16 h, the reaction was concentrated, dissolved in chloroform, and precipitated into hexanes twice, affording **HSp-DMAEMA** as a white solid. (299 mg, 66%. M<sub>n</sub>: 30 kDa, M<sub>w</sub>: 57 kDa) <sup>1</sup>H NMR (500 MHz, CDCl<sub>3</sub>): δ (ppm) 7.22-7.00, 6.90-6.78, 6.71-6.61, 5.77-5.63, 4.23-3.92, 3.60-3.30, 2.66-2.46, 2.43-2.39, 2.32-2.22, 2.16-2.13, 2.00-1.54, 1.44-0.77.

## HSp-AMPS

To a solution of **5** (52 mg, 0.14 mmol) in DMF (6 mL) was added AMPS (545 mg, 2.63 mmol) and AIBN (6 mg). The reaction mixture was fully dissolved by stirring for 15 minutes, and then degassed via three freeze-pump-thaw cycles. The reaction was heated at 65 °C under argon overnight. After 16 h, the reaction was cooled, precipitated into ethyl acetate, dissolved in deionized water, and dialyzed (MWCO 3.5 kDa) against deionized water for 2 d. The aqueous solution was concentrated under vacuum and dried via azeotropic distillation with ethanol, affording **HSp-AMPS** as an orange solid (206 mg, 35%. M<sub>n</sub>: 9 kDa, M<sub>w</sub>: 11 kDa). <sup>1</sup>H NMR (500 MHz, D<sub>2</sub>O): δ (ppm)8.82-8.50, 8.05-7.41, 7.20-6.77, 3.76-3.00, 2.34-0.73.

## OMeSp-PEGMA

PEGMA was eluted from a basic alumina plug to remove inhibitor. To a Schlenk flask was added 7 (58 mg, 0.14 mmol) in anhydrous THF (3.3 mL), PEGMA (0.78 mL, 2.7 mmol), EBiB (8.5  $\mu$ L, 0.057 mmol), and copper (I) bromide (8.2 mg, 0.057 mmol). The mixture was degassed via three freeze-pump-haw cycles. To the reaction mixture under argon was PMDETA (23.8  $\mu$ L, 0.114 mmol), which had been sparged with argon for 30 minutes. The reaction mixture was

heated at 65 °C overnight. After 16 h, the reaction was removed from heat and exposed to air. The reaction was diluted with  $CH_2Cl_2$ , filtered through a plug of neutral aluminum oxide, concentrated, and precipitated out of chloroform into hexanes twice, affording **OMeSp-PEGMA** as a gel. (493 mg, 56%.  $M_n$ : 16 kDa,  $M_w$ : 21 kDa) <sup>1</sup>H NMR (500 MHz, CDCl<sub>3</sub>):  $\delta$  (ppm) 7.19-7.10, 7.07-7.02, 6.88-6.59, 5.75-5.63, 4.31-3.88, 3.86-3.50, 3.39-3.36, 3.25-3.22, 2.05-1.67, 1.46-0.73.

## OMeSp-DMAEMA

To a solution of **7** (50 mg, 0.12 mmol) in toluene (4.2 mL) was added DMAEMA (0.39 mL, 2.3 mmol) and AIBN (4.2 mg). The reaction mixture was deoxygenated by sparging with argon for 25 min, and then heated at 65 °C overnight. After 16 h, the reaction mixture was cooled and concentrated. The residue was dissolved in chloroform and precipitated into hexanes twice, affording **OMeSp-DMAEMA** as a red solid. (272 mg, 65%. M<sub>n</sub>: 15 kDa, M<sub>w</sub>: 33 kDa) <sup>1</sup>H NMR (300 MHz, CDCl<sub>3</sub>): δ (ppm) 7.20-6.98, 6.87-6.55, 5.75-5.61, 4.36-3.77, 3.70-3.26, 2.83-2.70, 2.68-2.40, 2.38-2.10, 2.08-1.56, 1.52-0.64.

## OMeSp-AMPS

To a solution of **7** (37 mg, 0.09 mmol) in DMF (4 mL) was added AMPS (359 mg, 1.73 mmol) and AIBN (4 mg). The reaction mixture was fully dissolved by stirring for 15 minutes, and then sparged with Ar for 25 min. The reaction was heated at 65 °C under argon overnight. After 16 h, the reaction was cooled, precipitated from MeOH into diethyl ether twice, dissolved in DI water, and dialyzed (MWCO 3.5 kDa) against deionized water for 7 d. The aqueous solution was concentrated under vacuum and dried via azeotropic distillation with ethanol, affording **OMeSp-AMPS** as an orange solid (127 mg, 32%. M<sub>n</sub>: 11 kDa, M<sub>w</sub>: 17 kDa). <sup>1</sup>H NMR (500 MHz, D<sub>2</sub>O): δ (ppm) 8.83-8.43, 7.98-6.82, 4.18-3.69, 3.64-2.99, 2.36-0.73.

#### Determination of apparent pKa values

Solutions were prepared in 1 mM glycine, citrate, or phosphate buffer, depending on the pH: glycine for 1<pH<3, citrate for 3<pH<6, phosphate for 6<pH<9. Polymer concentrations for all solutions were 0.01% (w/v), and generally afforded a maximum absorbance around 0.5 OD between 400-450 nm for pH << pKa. Solutions were prepared and allowed to equilibrate at ambient temperature for at least 16 hours in the dark before measurement. For each polymer, absorbance spectra were measured in a range of different buffers at different values of pH. Solutions were kept in subdued lighting during this process. Apparent pKa values were determined from these data by plotting a titration curve of MCH<sup>+</sup> absorbance against pH.

## Extinction coefficients

Extinction coefficients were determined for each monomer in their respective PEGMA polymers. Total polymer spiropyran content was determined by quantitative <sup>1</sup>H NMR with reference to a known concentration of malic acid as an internal standard. Polymer solutions were prepared in DMSO-d<sub>6</sub>. Separately, polymer absorbance was measured at low pH (100 mM HCl) to induce maximal isomerization to the protonated species. From the concentration of SP measured using <sup>1</sup>H NMR, extinction coefficients were calculated based on application of the Beer-Lambert Law to absorbance values. Limited solubility of DMAEMA polymers in DMSO made their quantification difficult. However, relative integrations of monomers suggested minor differences in spiropyran extinction coefficients across different comonomers. Thus, extinction coefficients calculated for PEGMA polymers were used as universal values for each of the three spiropyran monomers appended to polymeric supports in water.

## Photochemical efficiencies of ring closing

All polymer samples for measurement of photochemical ring closure were prepared in 1 mM glycine buffer at pH 2. Polymer concentrations were adjusted to afford an absorbance of ~0.8 OD at  $\lambda_{max}$  at 400-450 nm for MCH<sup>+</sup>. Irradiations were performed with a 200 W Hg/Xe arc lamp, with one of three specific sets of conditions: (1) 3 mW/cm<sup>2</sup> using a 404 nm interference filter for determination of quantum yield, (2) 35 mW/cm<sup>2</sup> over the relevant wavelength range of 295< $\lambda$ <665 nm using a 295 nm long-pass filter for samples in which ring closure was slow or thermal ring opening fast enough to compete with the ring closure, and (3) 7 mW/cm<sup>2</sup> over the wavelength range 530< $\lambda$ <665 nm using a 530 nm long-pass filter for irradiation of samples with appreciable MC absorbance at thermal equilibrium in the dark. Samples were irradiated in cuvettes at a source to sample distance of 25 cm, with magnetic stirring. Absorbance measurements were made immediately following irradiation.

## Quantum yields of ring closing

Quantum yields of ring closure were determined through the application of Equation 1. Moles of photoproduct created was determined through the measurement of change in MCH<sup>+</sup> absorbance, held constant to approximately 15% decrease across all samples. Photon flux was determined immediately prior to each set of experiments, using the Parker actinometer.<sup>57</sup> Percent of light absorbed was determined from initial sample MCH<sup>+</sup> absorbance.

$$\Phi = \frac{(moles\ of\ photoproduct)}{(photon\ flux\ incident\ on\ sample)*(\%\ light\ absorbed\ by\ MCH+)} \tag{1}$$

## Rates of thermal ring opening

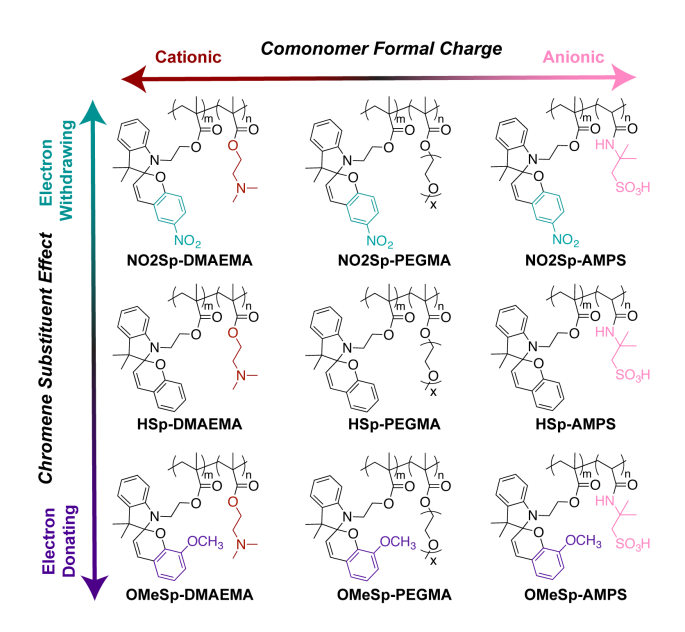
Absorbance was monitored at MCH<sup>+</sup>  $\lambda_{max}$  (400-450 nm) for each polymer, prepared as 0.01% w/v solutions in 1 mM glycine buffer (pH 2) or 1 mM citrate buffer (pH 6, for AMPS polymers). Initially, polymer solutions were exposed to 35 mW/cm<sup>2</sup> at  $\lambda > 295$  nm using a long-pass filter

for 10 minutes to induce ring-closure to the photostationary state. Immediately following irradiation, the sample was kept in the dark (except for those periods during acquisition of absorbance spectra), and recovery of MCH<sup>+</sup> was monitored by measuring absorbance spectra of the sample periodically until MCH<sup>+</sup> absorbance reached a plateau. Rate constants were determined by fitting each plot to an exponential function. Fatigue experiments were performed by repeated irradiation and thermal equilibration steps, recording the absorbances of MCH<sup>+</sup> after each step.

## Photoacidity experiments

Aqueous solutions of polymer, in the absence of any other buffering agent, were prepared to monitor changes in pH as a function of light exposure. Generally, 2.5% (w/v) polymer solutions were prepared in 0.1 M NaCl (aq). Both HCl (1 M) and NaOH (1 M) were used to adjust initial solution pH. Polymer solutions were subjected to 10-minute exposures to light ( $\lambda > 295$  nm, 35 mW/cm<sup>2</sup>) followed by extended periods of time in the dark. For **HSp-PEGMA** polymer experiments, irradiated solutions were held in dark for a minimum of 2 hours before continued use. For **HSp-AMPS** polymer experiments, irradiated solutions were held in dark for a minimum of 30 minutes before continued use. Extended storage in dark did not have an observed effect on solution pH for either polymer. Due to the fast recovery of solution pH for the AMPS polymers, pH measurements for these samples were performed under continued light exposure, after the initial 10-minute exposure. Then, upon removal of light, pH change was monitored as a function of time in the dark. Overall, ten irradiation-dark cycles were performed for both **HSp-PEGMA** and **HSp-AMPS** experiments.

**Chart 1.** Matrix of nine water-soluble spiropyran containing polymers prepared from combinations of three spiropyran methacrylates and three hydrophilic monomers of varying formal charge.



#### **Results and Discussion**

#### Experimental Design

We quantified the effects of polymer structure on three key properties of the photochromes: pKa values of MCH<sup>+</sup>, quantum yields of MCH<sup>+</sup> ring closure upon exposure to visible light, and rates of thermal recovery of MCH<sup>+</sup> in the dark. Unlike 'normal' spiropyran photochromism in hydrophobic environments, which is dominated by 6-nitrospiropyran derivatives, a greater diversity of spiropyran substitution patterns can yield reverse photochromism in water. We therefore selected three spiropyran substituent patterns on the chromene ring that varied both in substituent effect and regiochemistry (unsubstituted, 6-nitro, and 8-methoxy). In addition, given the influence that local electrostatic effects can have on acidity, we chose cationic (DMAEMA), neutral (PEGMA), and anionic (AMPS) comonomers. As shown in Chart 1, the resulting matrix of spiropyran-substituted water-soluble statistical copolymers, each of which comprised one of

three hydrophilic comonomers and one of three spiropyran derivatives, yielded nine polymers with unique physical and chemical properties.

## Polymer Synthesis

Spiropyran-methacrylate monomers were synthesized according to a previously reported procedure. 56 As shown in Scheme 1, formation of the spiropyran alcohols 2, 4, 6 proceeded with the only difference between monomers being the salicylaldehyde derivative used in the condensation step. Acylation of the spiropyran alcohols with methacryloyl chloride afforded the monomers 3, 5, 7, which were amenable to purification through chromatography, recrystallization, or a combination of the two. Polymers were prepared as statistical copolymers between two monomers: 5 mole-percent of a spiropyran monomer, and 95 mole-percent of a water-solubilizing comonomer. We used atom-transfer radical polymerization (ATRP) to prepare PEGMA-based polymers, and AIBN-initiated free-radical polymerization to prepare AMPS- and DMAEMA-based polymers. AMPS polymers required dialysis against deionized water to remove unreacted monomer. Generally, these reactions yielded polymers with number-average molecular weights (Mn) between 10-35 kDa, with PDIs ≤ 2.1 for AIBN polymerizations and ≤ 1.6 for ATRP, as determined by gel permeation chromatography. AMPS polymers displayed low PDIs (≤ 1.6) due to fractionation during dialysis. We determined by <sup>1</sup>H NMR spectroscopy that the typical SP composition of isolated polymers was ~3-4 mole-percent. The PEGMA and AMPS polymers dissolved in water readily, while DMAEMA polymers did so upon acidification and sonication.

#### Apparent pKa Values of MCH<sup>+</sup>

The pKa of MCH+ is important because it determines the pH values at which photoinduced change in pH can be realized. MCH<sup>+</sup> is generally the more stable form of the spiropyran

photochrome when pH < pKa. The equilibrium shifts towards SP at higher pH, indicated by a decrease in the MCH<sup>+</sup> absorbance around 430 nm, and an increase in absorbance below 300 nm (*Figure 2, top*). With several exceptions (*vide infra*), the MC species was transient for most polymers in solution, at any pH, and could only be observed immediately upon addition of base to an acidic solution of MCH<sup>+</sup>. <sup>19,43</sup>

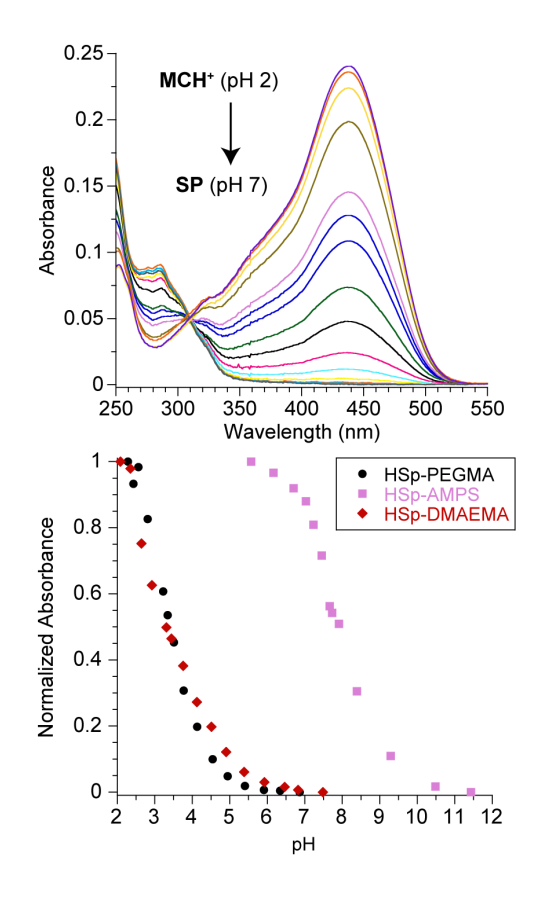


**Figure 2.** Determination of apparent pKa of MCH<sup>+</sup> in polymers with unsubstituted spiropyran pendants. Top: Solution absorbance spectra in buffers of various pH values for **HSp-PEGMA** (2<pH<7). Bottom: Comparison of pH titration curves for **HSp-**pendant polymers with different hydrophilic comonomers. The overall trend observed was that more electron rich chromene rings and negatively charged comonomers yielded less acidic MCH<sup>+</sup> groups.

Experimental Approach: Analysis of absorbance spectra of each polymer in buffers at a range of pH values provided apparent pKa values for the MCH<sup>+</sup> side chains of each polymer. As equilibration between the SP and MCH<sup>+</sup> states is not instantaneous, solutions were placed in the dark until their spectra showed no changes in absorbance before measurement for apparent pKa determination. Figure 2 (bottom) shows examples of titration curves for each of the unsubstituted spiropyrans (HSp) with different comonomers. By measuring MCH<sup>+</sup> absorbance over a range of pH values, we determined the relative amounts of MCH<sup>+</sup> present with respect to fully protonated (low pH) and fully deprotonated (high pH) states. We take the pH values for which 50% of the maximal MCH<sup>+</sup> absorbance occurs as apparent MCH<sup>+</sup> pKa values, at which half of the population of the photochrome exists in the ionized form.

Observed Trends: Two clear structure-acidity trends emerge from an analysis of the apparent pKa values listed in Table 1. First, the substituents on the chromene ring of the spiropyran influenced pKa. In accordance with reported literature, increasing electron density in the chromene ring decreases the acidity of the MCH<sup>+</sup> phenol.<sup>54</sup> While this trend generally holds in each case, this effect is most pronounced for the PEGMA polymers, listed in Table 1. This follows chemical intuition, since electron-withdrawing nitro groups best stabilize the conjugate base. Second, the structure of the hydrophilic comonomer influenced MCH<sup>+</sup> acidity. This effect is particularly pronounced for the AMPS polymers, displaying an increase in apparent acid dissociation constant of at least three orders of magnitude from PEGMA- to AMPS-based polymers for each of the three spiropyran moieties examined. Following a known general trend of polymeric acids, the anionic environment decreases acid strength of the MCH<sup>+</sup> phenol. Importantly, the observed pKa values of the MCH<sup>+</sup> moieties of the AMPS-based polymers fall in a range of biological significance, spanning from values of 6.4-7.6. MCH<sup>+</sup> moieties of the other

polymers are almost entirely deprotonated in this range of pH, and therefore favor SP forms and are unlikely to show negative photochromism under such conditions.

Table 1. Photochromism parameters of the nine spiropyran-substituted polymers in water

		pKa'	□°	k <sub>pH 2</sub> (s <sup>-1</sup> )	k <sub>pH 6</sub> (s <sup>-1</sup> )	Fraction SP at PSS <sub>pH 2</sub>	Fraction SP at PSS pH 6
PEGMA	$NO_2$	2.3	0.19	$2.4 \times 10^{-5}$		$0.97^{a}$	
	H	3.4	0.18	$1.1 \times 10^{-4}$		$0.96^{a}$	
	OMe	4.1		$(>10^{-3})$		$0.04^{a}, 0.41^{b}$	
DMAEMA	$NO_2$	2.4	0.16	$7.9 \times 10^{-5}$		$0.90^a, (0.93^b)$	
	H	3.4	0.15	$2.8 \times 10^{-3}$		$0.53^{a}, 0.90^{b}$	
	OMe	3.4				$0.02^{b}$	
AMPS	$NO_2$	6.4	0.20	$1.4 \times 10^{-5}$	$5.2x10^{-5}$	$0.67^{a}, 0.56^{b}$	$0.73^{a}, 0.76^{b}$
	H	7.6	0.17	$2.4 \times 10^{-4}$	$3.9x10^{-3}$	$0.49^{a}, 0.52^{b}$	$0.36^{a}, 0.82^{b}$
	OMe	7.4		$(>10^{-3})$		$0.01^{a}, 0.04^{b}$	$0.01^{a}, 0.04^{b}$

<sup>&</sup>lt;sup>a</sup> interference filter ( $\lambda$  = 404 nm, 3 mW/cm<sup>2</sup>) <sup>b</sup> long pass filter ( $\lambda$  > 295 nm, 35 mW/cm<sup>2</sup>) <sup>c</sup> MCH<sup>+</sup> → SP (pH 2)

#### Photochemical Ring Closure

Experimental Approach: The reversible, photoinduced ring closure of MCH<sup>+</sup> to SP is important because it both changes the color of the sample from yellow to colorless (negative photochromism) and changes the formal charge of the photochrome by releasing protons into the environment. We therefore determined how the changes in chemical structure of our nine polymers influence the quantum yields of these reactions. Due to the expected low pKa (< 2) of the ammonium cation of ring-closed SP (SPH<sup>+</sup>),<sup>17</sup> MCH<sup>+</sup> and SP species were considered the major components present in the pH range used in these experiments (2<pH<6). We investigated the structure-property relationships of this reaction under two different sets of conditions. Since MCH<sup>+</sup> absorbs 400-450 nm, we irradiated with these colors of blue light to induce ring closing reactions (Figure 3). Quantum yields were calculated for sufficiently fast ring-closing polymers utilizing a 404 nm (+/- 20 nm) interference filter with power density of 3 mW/cm<sup>2</sup> (Table 1). For

OMeSp polymers, however, the reverse, thermal ring-opening reactions were too fast to accurately determine quantum yields. Therefore, these samples were irradiated with light of greater intensity using a long-pass filter ( $\lambda > 295$  nm) at a power density of 35 mW/cm<sup>2</sup> in the relevant wavelength range, as a point of comparison.

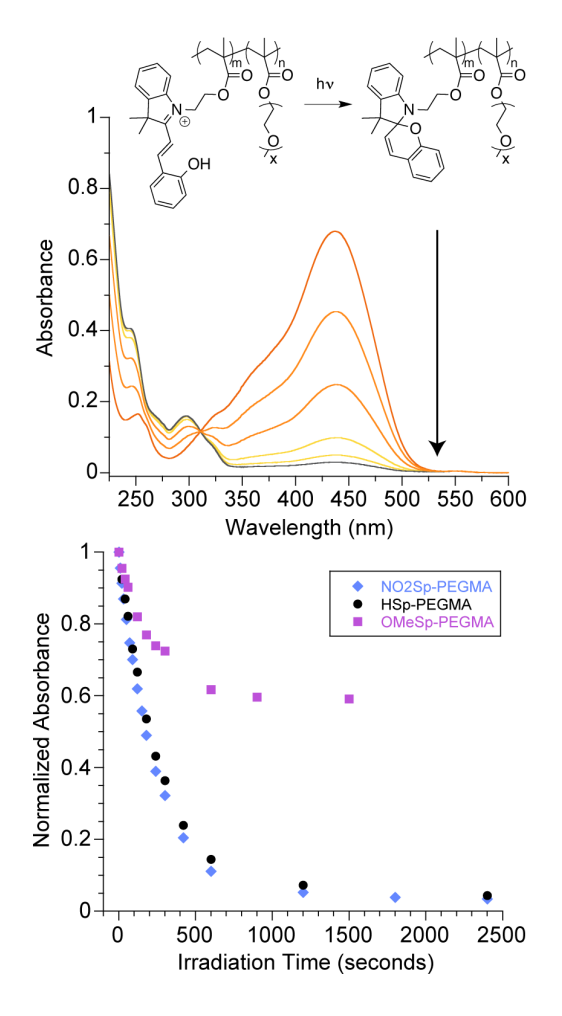


**Figure 3:** Top: Decrease in MCH<sup>+</sup> absorbance of **HSp-PEGMA** exposure to 404 nm, 3 mW/cm<sup>2</sup> at irradiation times 0 min, 2 min, 5 min, 10 min, 15 min, 25 min. Bottom: Comparison of the ring closure kinetics of all three PEGMA polymers in pH 2 buffer. **NO<sub>2</sub>Sp-** and **HSp-PEGMA** were irradiated at 404 nm (3 mW/cm<sup>2</sup>), while **OMeSp-PEGMA** required more intense irradiation ( $\lambda$  > 295 nm, 35 mW/cm<sup>2</sup>) to induce ring closing.

Observed Trends: Substituents on the chromene moiety of the photochromes have noticeable effects on ring closing rates. While NO₂Sp polymers generally had the highest quantum yields of ring closure (□), both the NO₂Sp and HSp polymers underwent efficient ring closure with quantum yields ranging from 0.1-0.2. On the contrary, polymers containing the OMeSp derivative had the slowest observed ring closing reactions, which we attribute in large part to rapid thermal ring opening that resulted in photostationary states that always had at least 50% of the MCH⁺ species still present in the ring open form. This rapid ring opening precluded measurement of □ for OMeSp polymers.

To quantify this observation, the photostationary states of each of the polymers upon irradiation at 35 mW/cm² and 3 mW/cm² visible light were determined (*Table 1*), which highlighted a number of key points. First, **OMeSp-DMAEMA** and **OMeSp-AMPS** displayed little observable (4%) change in (MCH†) absorbance upon 10-minute irradiation, even at 35 mW/cm², indicating rapid thermal reversion back to MCH†. Second, in typical experiments, increasing the incident light intensity would increase the extent of ring closure at the PSS. However, for **HSp-AMPS** at pH 2, both high and low light intensities induced ~50% ring closure at the PSS. We suspect that these values represent near complete conversion of MCH† to SP, but the existence of additional protonated species (SpH†) at this low pH limits the amount of isomerization possible through irradiation alone. For **NO<sub>2</sub>Sp-AMPS** at pH 2, increased light intensity even resulted in less ring closure at the PSS, which we suspect is a result of the wider wavelength range of the 295 nm long pass filter used, resulting in light-induced reversion.

Polymers with MC at equilibrium: Interestingly, several polymers exhibited all three species – SP, MCH<sup>+</sup>, and MC – at equilibrium. Specifically, nitro-substituted spiropyrans (NO<sub>2</sub>Sp) polymerized with ionic comonomers afforded a highly polar environment in which MC could be

stabilized to a greater extent than in the PEGMA polymers. Exposure of a solution of  $NO_2Sp$ DMAEMA to 404 nm light at pH 2 lead to a simultaneous decrease in both MCH<sup>+</sup> and MC
absorbance bands (*Figure S1*). In agreement with a previous observation from Liao et al.<sup>23</sup>,
exposure of a sample solution to  $\lambda > 530$  nm light (7 mW/cm<sup>2</sup>) also decreased concentration of
both ring open forms, as demonstrated in Figure 4. Negative photochromism of the MCH<sup>+</sup>
isomer was therefore observed with an excitation wavelength over 100 nm red-shifted from
typical MCH<sup>+</sup> absorbance. A control experiment with  $NO_2Sp$ -AMPS, which exhibits less MC
absorbance between 500-600 nm relative to MCH<sup>+</sup> at equilibrium at pH 2 showed far slower
change in MCH<sup>+</sup> and MC absorbance upon identical irradiation at  $\lambda > 530$  nm.(*Figure 4*,
bottom).

A second consequence of the existence of the MC species at equilibrium is the possibility for hydrolytic degradation over time, since it is more susceptible to nucleophilic attack by water than MCH<sup>+</sup>.<sup>17</sup> Among the nine polymers studied here, polymeric solutions that showed appreciable MC absorbance degraded over time, displaying a decrease in MCH<sup>+</sup> and MC absorbance. Since NO<sub>2</sub>Sp-DMAEMA exhibits MC over a wide pH range (due to a low MCH<sup>+</sup> pKa of 2.4), sample degradation is observed continuously over time, even at low pH (pH 2, *Figure S2*). However, in the case of NO<sub>2</sub>Sp-AMPS, MC absorbance can be reduced to zero over the pH range of study (2 < pH < 7). At pH 2, the sample resisted degradation due to the full protonation of MC to MCH<sup>+</sup>. However, at pH 6, the existence of MC at equilibrium resulted in susceptibility to hydrolysis (*Figure S3-S4*).

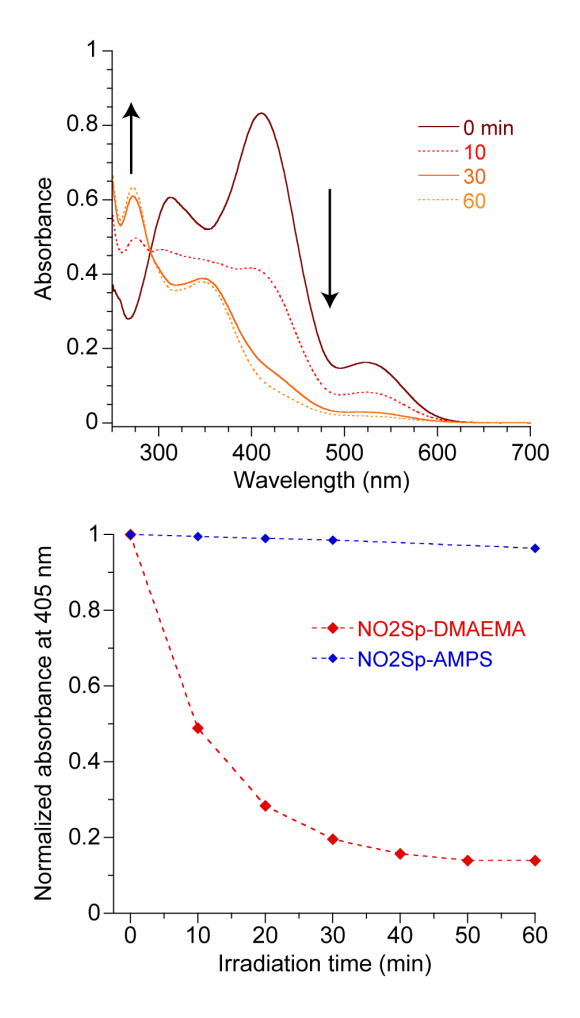


**Figure 4.** Photochemical ring closing of MC and MCH<sup>+</sup> upon irradiation of only MC isomer at 

□ > 530 nm, 7 mW/cm<sup>2</sup>. *Top*: Absorbance spectra of **NO<sub>2</sub>Sp-DMAEMA** (pH 2) during irradiation at □ > 530 nm. *Bottom*: Conversion from MCH<sup>+</sup> to SP upon irradiation at □ > 530 nm is ineffective for the AMPS polymer analog at pH 2, which shows almost no absorbance attributed to the MC derivative.

## Isomerization Rates

Experimental Approach: We also determined substituent effects for thermal ring opening from SP to MCH<sup>+</sup> for the series of polymers. Before measuring the kinetics of ring opening, we exposed aqueous samples to  $\lambda > 295$  nm (35 mW/cm<sup>2</sup>) for 10 minutes, to promote ring closure to

PSS for all samples. Exceptions to this procedure were **OMeSp-DMAEMA** and **OMeSp-AMPS** polymers since they did not exhibit substantial ring closure at the PSS, forming less than 5% of SP from MCH<sup>+</sup>.

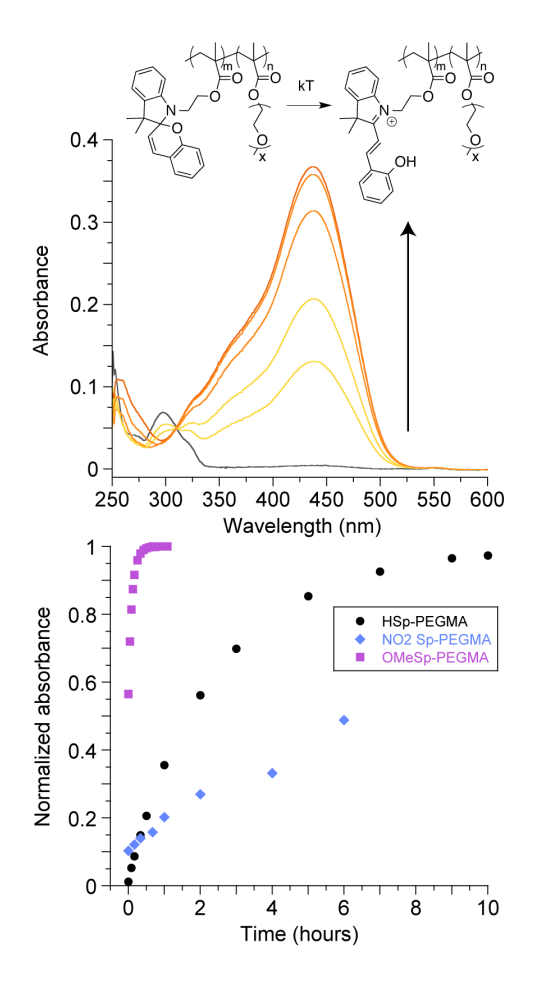


**Figure 5.** Top: Recovery of MCH<sup>+</sup> absorbance of **HSp-PEGMA** following irradiation at ambient temperature. Spectra correspond to the following total times in dark: 0 hr, 1 hr, 2 hr, 5 hr, 10 hr, 24 hr. Bottom: Comparison of thermal ring-opening rates amongst PEGMA polymers. Overall, 8-methoxy-substituted spiropyrans recovered MCH<sup>+</sup> fastest, while 6-nitro-substituted spiropyrans recovered MCH<sup>+</sup> slowest.

Observed Trends: Thermal ring opening rates of these polymers correlated closely with chemical structure (*Figure 5*). With respect to substituent effects on the spiropyran moiety itself, nitro-substituted spiropyrans exhibited the slowest thermal ring opening of any of the polymers, in the case of NO<sub>2</sub>Sp-PEGMA requiring over 72 hours in the dark to recover the original MCH<sup>+</sup> absorbance with a rate constant of 2.4x10<sup>-5</sup> s<sup>-1</sup>. In contrast, the OMeSp polymers recovered complete MCH<sup>+</sup> absorbance in fewer than 60 minutes at room temperature with rate constants of at least 1x10<sup>-3</sup> s<sup>-1</sup>. This observation aligns most closely with previous work reported by Zhou et al., who concluded that the rate determining step of the acid-induced ring opening was between a protonated, positively charged "species Y" and the final product MCH<sup>+</sup>, which necessitates the existence of some character of the protonated phenol in the rate determining transition state.<sup>58</sup> This is an important difference between the mechanisms of normal and reverse photochromism observed for spiropyrans, and contributes to the large changes in behavior of different spiropyran derivatives in water and organic media.

Comonomer structure also influenced thermal ring opening rates. Comparing the rates for HSp polymers, which were the most tunable on practical times-scales, the ring-opening of spiropyrans copolymerized with charged comonomers (AMPS, DMAEMA) ring-opened an order of magnitude faster than those with PEGMA comonomer (~10<sup>-3</sup> vs. ~10<sup>-4</sup>, respectively) resulting in the times required for complete thermal recovery ranged from under 60 minutes to approximately 8 hours. We suspect that the PEGMA pendants stabilize the hydrophobic SP to the greatest extent of the three comonomers, while the ionic pendants stabilize preferentially a polar transition state, accounting for a small activation barrier to ring opening for DMAEMA and AMPS, and a comparatively larger one for PEGMA.

Altogether, the polymers containing the HSp derivative were the most tunable on practical time scales. Importantly, these buffered solutions of negatively photochromic polymers resisted photochemical fatigue. As seen in Figure 6, subjection of all three HSp polymers to 15 irradiation cycles (10 minutes, 35 mW/cm<sup>2</sup>,  $\lambda > 295$  nm) lead to a maximum decrease of 2% in MCH<sup>+</sup> absorbance after thermal recovery. This is in agreement with known photo-induced fatigue resistance for the MCH<sup>+</sup> to SP transition.<sup>59</sup>

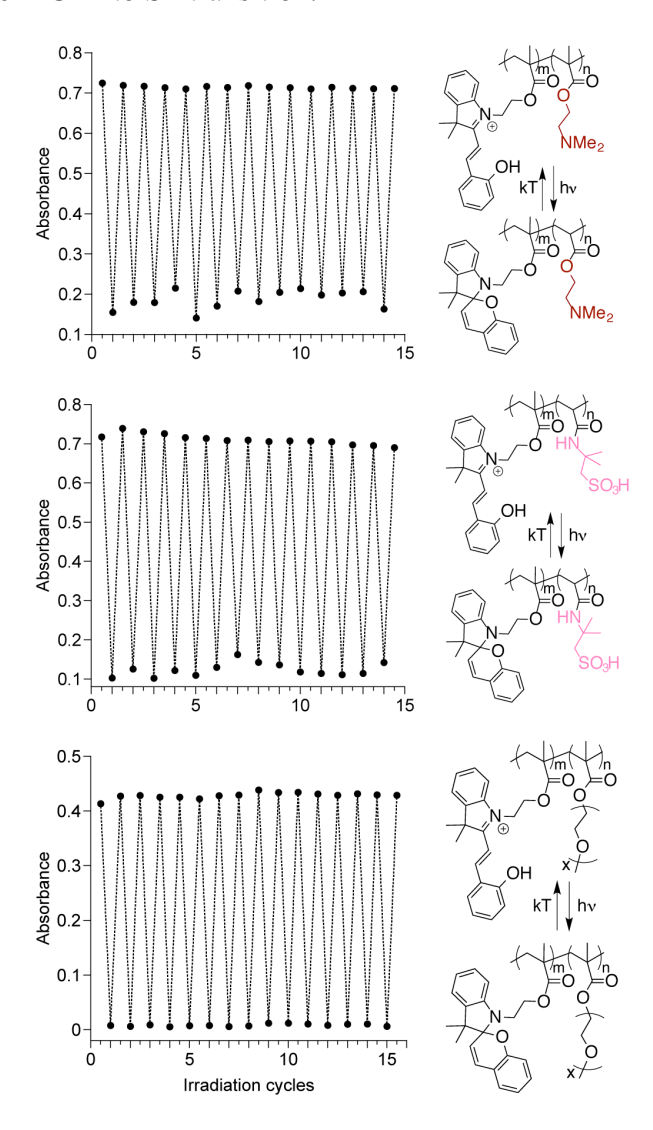


**Figure 6.** Fatigue resistance of HSp-pendant polymers during 10-min irradiation cycles at  $\lambda > 295$  nm, 35 mW/cm<sup>2</sup>, and subsequent thermal recovery. Absorbance was monitored at  $\lambda_{max}$  between 400-450 nm.

We noted strong pH dependence for the rate constants and PSS composition for AMPS polymers. The effect is highlighted by the increase in rate constant of ring opening for HSp-AMPS by an order of magnitude from pH 2 to pH 6. Preliminarily, we attribute this effect to anionic sulfonate groups increasing pKa of both MCH<sup>+</sup> and protonated nitrogen on the spiropyran indoline (SPH<sup>+</sup>), a species that does not undergo isomerization until after deprotonation.<sup>60</sup> This observation highlights a key point – the most effective photoacid range for the AMPS polymer is near the MCH<sup>+</sup> pKa (pH 5-7), since it is in this range that the polymers exhibit the most efficient isomerization (both in terms of rates and extent of ring closure at the photostationary state). The same is true for the PEGMA polymer, and since the pKa is lower for this polymer, the effective pH range is also lower. Thus, comonomer choice can dictate photoacid function of the various SP species based on the pH range of the target application.

## Reversible Photoacidity

The increase in acidity for MCH<sup>+</sup> to SP upon ring closure allows for the light-induced release of protons into solution. This process yields reversible pH changes that can be visualized by combination with pH indicators.<sup>25,26,28</sup> While this reaction is known to modulate pH in various platforms, typically the effective pH range is dictated by the structure of the photochrome itself. Here we demonstrate the reversible photoacidity of two polymers that bear the same spiropyran, unsubstituted on the chromene moiety. Figure 7 shows the reversible pH response of **HSp-PEGMA** and **HSp-AMPS** polymers dissolved in 0.1 M NaCl (10 mg/mL). For both polymers, exposure to light of  $\lambda > 295$  nm (35 mW/cm<sup>2</sup>) for 10 minutes yielded a decrease in solution pH of 0.2 to 0.6 units. This photoinduced solution pH returned to pre-irradiation values as the SP unit re-opened to MCH<sup>+</sup> at room temperature.

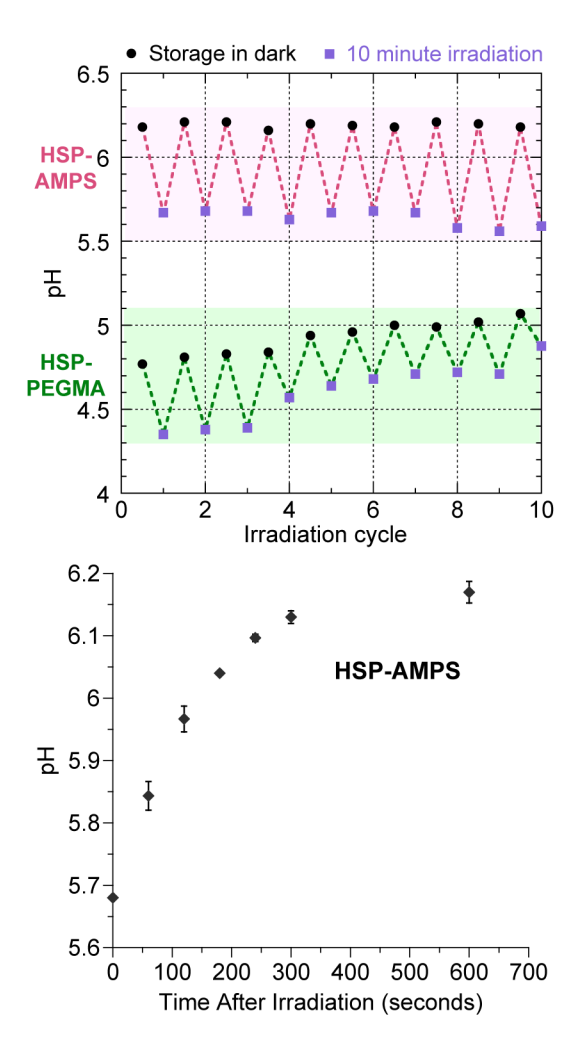


**Figure 7.** *Top*: **HSp-AMPS** shows photo-switchable pH at higher pH values than **HSp-PEGMA** due to electrostatic effects of the anionic co-monomer. *Bottom:* Return of pH to pre-irradiation value following irradiation of **HSp-AMPS.** The data points show the average of three independent trials, while the error bars represent one standard deviation.

Because of its higher pKa, **HSp-AMPS** showed photoacidic activity closer to neutral pH than **HSp-PEGMA**, despite the fact that the photochromic monomer is the same in both polymers. As a control experiment, a solution of **HSp-PEGMA** solution at pH 6.1 exhibited inconsistent pH changes that did not exceed differences of 0.1 (*Figure S5*). Moreover, the rapid equilibration of

irradiated **HSp-AMPS** resulted in recovery of original pH values in less than 30 minutes. Similar behavior was observed for solutions with no added NaCl (*Figure S6*). This rapid rate of recovery, in combination with the elevated effective pH range, establishes **HSp-AMPS** as an intriguing photoacid for further study.

#### Conclusion

That spiropyran-based materials can access three different species—SP, MC, and MCH<sup>+</sup>—is a powerful tool for switchable materials. This paper demonstrates how the modular design of copolymers not only allows water solubilization of a hydrophobic spiropyran unit, but also enables broad tuning of its photochromic properties. In this work, we demonstrated chemically decoupled modifications of the photochromic efficiencies, which depended here mostly on the structure of the spiropyran moiety itself, from the apparent acidity of the MCH<sup>+</sup> photoacid, which the electrostatic environment provided by the hydrophilic co-monomer could tune up to 3-4 orders of magnitude. Moreover, we note that the fatigue resistance of these photochromic polymers improved when we used buffered solutions, as opposed to simply protonating the MCH<sup>+</sup> with strong acid. Analysis of negative photochromism in buffered solutions is also likely to be more relevant to future biological applications.

#### ASSOCIATED CONTENT

**Supporting Information**. The following files are available free of charge.

PDF file containing NMR spectra of new monomers and polymers, raw absorbance data for pKa, quantum yield, and rate constant determination, supporting figures

#### **AUTHOR INFORMATION**

# **Corresponding Author**

\* Email: sam.thomas@tufts.edu

#### **Funding Sources**

This material is based upon work supported by the National Science Foundation under Awards CHE-1806263 and DMR-1151385.

#### **REFERENCES**

- 1. Cohen Stuart, M. A.; Huck, W. T. S.; Genzer, J.; Muller, M.; Ober, C.; Stamm, M.; Sukhorukov, G. B.; Szleifer, I.; Tsukruk, V. V.; Urban, M.; Winnik, F.; Zauscher, S.; Luzinov, I.; Minko, S. Emerging Applications of Stimuli-Responsive Polymer Materials. *Nat. Mater.* **2010**, *9*, 101-113.
- 2. Roy, D.; Cambre, J. N.; Sumerlin, B. S. Future Perspectives and Recent Advances in Stimuli-Responsive Materials. *Prog. Polym. Sci.* **2010**, *35*, 278-301.
- 3. Mura, S.; Nicolas, J.; Couvreur, P. Stimuli-Responsive Nanocarriers for Drug Delivery. *Nat. Mater.* **2013**, *12*, 991-1003.
- 4. Richter, A.; Paschew, G.; Klatt, S.; Lienig, J.; Arndt, K. F.; Adler, H. J. P. Review on Hydrogel-Based pH Sensors and Microsensors. *Sensors* **2008**, *8*, 561-581.
- 5. Miller, E. W.; Bian, S. X.; Chang, C. J. A Fluorescent Sensor for Imaging Reversible Redox Cycles in Living Cells. *J. Am. Chem. Soc.* **2007**, *129*, 3458-3459.
- 6. Raymo, F. M.; Alvarado, R. J.; Giordani, S.; Cejas, M. A. Memory Effects Based on Intermolecular Photoinduced Proton Transfer. *J. Am. Chem. Soc.* **2003**, *125*, 2361-2364.
- 7. Ercole, F.; Davis, T. P.; Evans, R. A. Photo-Responsive Systems and Biomaterials: Photochromic Polymers, Light-Triggered Self-Assembly, Surface Modification, Fluorescence Modulation and Beyond. *Polym. Chem.* **2010**, *1*, 37-54.
- 8. Hansen, M. J.; Velema, W. A.; Lerch, M. M.; Szymanski, W.; Feringa, B. L. Wavelength-Selective Cleavage of Photoprotecting Groups: Strategies and Applications in Dynamic Systems. *Chem. Soc. Rev.* **2015**, *44*, 3358-3377.

- 9. Kaur, G.; Johnston, P.; Saito, K. Photo-Reversible Dimerisation Reactions and Their Applications in Polymeric Systems. *Polym. Chem.* **2014**, *5*, 2171-2186.
- 10. Russew, M. M.; Hecht, S. Photoswitches: From Molecules to Materials. *Adv. Mater.* **2010**, 22, 3348-3360.
- 11. Berkovic, G.; Krongauz, V.; Weiss, V. Spiropyrans and Spirooxazines for Memories and Switches. *Chem. Rev.* **2000**, *100*, 1741-1753.
- 12. Irie, M. Diarylethenes for Memories and Switches. Chem. Rev. 2000, 100, 1685-1716.
- 13. Yokoyama, Y. Fulgides for Memories and Switches. Chem. Rev. 2000, 100, 1717-1739.
- 14. Klajn, R. Spiropyran-Based Dynamic Materials. Chem. Soc. Rev. 2014, 43, 148-184.
- 15. Moldenhauer, D.; Grohn, F. Water-Soluble Spiropyrans with Inverse Photochromism and Their Photoresponsive Electrostatic Self-Assembly. *Chem. Eur. J.* **2017**, *23*, 3966-3978.
- 16. Stafforst, T.; Hilvert, D. Kinetic Characterization of Spiropyrans in Aqueous Media. *Chem. Commun.* **2009**, 287-288.
- 17. Hammarson, M.; Nilsson, J. R.; Li, S. M.; Beke-Somfai, T.; Andreasson, J. Characterization of the Thermal and Photoinduced Reactions of Photochromic Spiropyrans in Aqueous Solution. *J. Phys. Chem. B* **2013**, *117*, 13561-13571.
- 18. Florea, L.; Diamond, D.; Benito-Lopez, F. Photo-Responsive Polymeric Structures Based on Spiropyran. *Macrolmol. Mater. Eng.* **2012**, 297, 1148-1159.
- 19. Sumaru, K.; Kameda, M.; Kanamori, T.; Shinbo, T. Reversible and Efficient Proton Dissociation of Spirobenzopyran-Functionalized Poly(*N*-isopropylacrylamide) in Aqueous Solution Triggered by Light Irradiation and Temporary Temperature Rise. *Macromolecules* **2004**, *37*, 7854-7856.
- 20. Aiken, S.; Edgar, R. J. L.; Gabbutt, C. D.; Heron, B. M.; Hobson, P. A. Negatively Photochromic Organic Compounds: Exploring the Dark Side. *Dyes Pigments* **2018**, *149*, 92-121.
- 21. Sumaru, K.; Takagi, T.; Satoh, T.; Kanamori, T. Photo-Induced Reversible Proton Dissociation of Spirobenzopyran in Aqueous Systems. *J. Photochem. Photobiol. A* **2013**, *261*, 46-52.
- 22. Chen, H. B.; Liao, Y. Photochromism Based on Reversible Proton Transfer. *J. Photochem. Photobiol. A* **2015**, *300*, 22-26.
- 23. Shi, Z.; Peng, P.; Strohecker, D.; Liao, Y. Long-Lived Photoacid Based Upon a Photochromic Reaction. *J. Am. Chem. Soc.* **2011**, *133*, 14699-14703.

- 24. Yang, C.; Khalil, T.; Liao, Y. Photocontrolled Proton Transfer in Solution and Polymers Using a Novel Photoacid with Strong C-H Acidity. *RSC Adv.* **2016**, *6*, 85420-85426.
- 25. Khalil, T.; Alharbi, A.; Baum, C.; Liao, Y. Facile Synthesis and Photoactivity of Merocyanine-Photoacid Polymers. *Macromol. Rapid Commun.* **2018**, *39*, 201800319.
- 26. Vallet, J.; Micheau, J. C.; Coudret, C. Switching a Ph Indicator by a Reversible Photoacid: A Quantitative Analysis of a New Two-Component Photochromic System. *Dyes Pigments* **2016**, *125*, 179-184.
- 27. Kundu, P. K.; Samanta, D.; Leizrowice, R.; Margulis, B.; Zhao, H.; Borner, M.; Udayabhaskararao, T.; Manna, D.; Klajn, R. Light-Controlled Self-Assembly of Non-Photoresponsive Nanoparticles. *Nat. Chem.* **2015**, *7*, 646-652.
- 28. Zhang, T.; Sheng, L.; Liu, J. N.; Ju, L.; Li, J. H.; Du, Z.; Zhang, W. R.; Li, M. J.; Zhang, S. X. A. Photoinduced Proton Transfer between Photoacid and Ph-Sensitive Dyes: Influence Factors and Application for Visible-Light-Responsive Rewritable Paper. *Adv. Funct. Mater.*

**2018**, 28, 1705332.

- 29. Samanta, D.; Galaktionova, D.; Gemen, J.; Shimon, L. J. W.; Diskin-Posner, Y.; Avram, L.; Kral, P.; Klajn, R. Reversible Chromism of Spiropyran in the Cavity of a Flexible Coordination Cage. *Nat. Commun.* **2018**, *9*, 641.
- 30. Wang, Z. Z.; Liao, Y. Reversible Dissolution/Formation of Polymer Nanoparticles Controlled by Visible Light. *Nanoscale* **2016**, *8*, 14070-14073.
- 31. Samanta, D.; Klajn, R. Aqueous Light-Controlled Self-Assembly of Nanoparticles. *Adv. Opt. Mater.* **2016**, *4*, 1373-1377.
- 32. Kundu, P. K.; Das, S.; Ahrens, J.; Klajn, R. Controlling the Lifetimes of Dynamic Nanoparticle Aggregates by Spiropyran Functionalization. *Nanoscale* **2016**, *8*, 19280-19286.
- 33. Jansze, S. M.; Cecot, G.; Severin, K. Reversible Disassembly of Metallasupramolecular Structures Mediated by a Metastable- State Photoacid. *Chem. Sci.* **2018**, *9*, 4253-4257.
- 34. Fu, C. K.; Xu, J. T.; Boyer, C. Photoacid-Mediated Ring Opening Polymerization Driven by Visible Light. *Chem. Commun.* **2016**, *52*, 7126-7129.
- 35. Li, X. B.; Fei, J. B.; Xu, Y. Q.; Li, D. X.; Yuan, T. T.; Li, G. L.; Wang, C. L.; Li, J. B. A Photoinduced Reversible Phase Transition in a Dipeptide Supramolecular Assembly. *Angew. Chem. Int. Ed.* **2018**, *57*, 1903-1907.

- 36. Maity, C.; Hendriksen, W. E.; van Esch, J. H.; Eelkema, R. Spatial Structuring of a Supramolecular Hydrogel by Using a Visible-Light Triggered Catalyst. *Angew. Chem. Int. Ed.* **2015**, *54*, 998-1001.
- 37. Shafaat, O. S.; Winkler, J. R.; Gray, H. B.; Dougherty, D. A. Photoactivation of an Acid-Sensitive Ion Channel Associated with Vision and Pain. *Chembiochem* **2016**, *17*, 1323-1327.
- 38. Luo, Y.; Wang, C. M.; Peng, P.; Hossain, M.; Jiang, T. L.; Fu, W.; Liao, Y.; Su, M. Visible Light Mediated Killing of Multidrug-Resistant Bacteria Using Photoacids. *J. Mater. Chem. B* **2013**, *1*, 997-1001.
- 39. Zhou, Y. N.; Zhang, Q.; Luo, Z. H. A Light and Ph Dual-Stimuli-Responsive Block Copolymer Synthesized by Copper(0)-Mediated Living Radical Polymerization: Solvatochromic, Isomerization, and "Schizophrenic" Behaviors. *Langmuir* **2014**, *30*, 1489-1499.
- 40. Zhang, Y.; Cao, M. J.; Yuan, B.; Guo, T. Y.; Zhang, W. Q. Raft Synthesis and Micellization of a Photo-, Temperature- and pH-Responsive Diblock Copolymer Based on Spiropyran. *Polym. Chem.* **2017**, *8*, 7325-7332.
- 41. Wu, Z.; Pan, K.; Lu, B. Z.; Ma, L.; Yang, W. T.; Yin, M. Z. Tunable Morphology of Spiropyran Assemblies: From Nanospheres to Nanorods. *Chem. Asian J.* **2016**, *11*, 3102-3106.
- 42. Xie, X. J.; Mistlberger, G.; Bakker, E. Reversible Photodynamic Chloride-Selective Sensor Based on Photochromic Spiropyran. *J. Am. Chem. Soc.* **2012**, *134*, 16929-16932.
- 43. Sumaru, K.; Kameda, M.; Kanamori, T.; Shinbo, T. Characteristic Phase Transition of Aqueous Solution of Poly(*N*-isopropylacrylamide) Functionalized with Spirobenzopyran. *Macromolecules* **2004**, *37*, 4949-4955.
- 44. Ivanov, A. E.; Eremeev, N. L.; Wahlund, P. O.; Galaev, I. Y.; Mattiasson, B. Photosensitive Copolymer of *N*-Isopropylacrylamide and Methacryloyl Derivative of Spyrobenzopyran. *Polymer* **2002**, *43*, 3819-3823.
- 45. Achilleos, D. S.; Vamvakaki, M. Multiresponsive Spiropyran-Based Copolymers Synthesized by Atom Transfer Radical Polymerization. *Macromolecules* **2010**, *43*, 7073-7081.
- 46. Sumaru, K.; Takagi, T.; Satoh, T.; Kanamori, T. Photo- and Thermoresponsive Dehydration of Spiropyran-Functionalized Polymer Regulated by Molecular Recognition. *Macromol. Rapid Commun.* **2018**, *39*, 1700234

- 47. Shiraishi, Y.; Sumiya, S.; Manabe, K.; Hirai, T. Thermoresponsive Copolymer Containing a Coumarin-Spiropyran Conjugate: Reusable Fluorescent Sensor for Cyanide Anion Detection in Water. *ACS Appl. Mater. Interf.* **2011**, *3*, 4649-4656.
- 48. Nagasawa, M., *Physical Chemistry of Polyelectrolyte Solutions*. Wiley-Blackwell: Hoboken, New Jersey, 2015.
- 49. Kotin, L.; Nagasawa, M. Chain Model for Polyelectrolytes. VII. Potentiometric Titration and Ion Binding in Solutions of Linear Polyelectrolytes. *J. Chem. Phys.* **1962**, *36*, 873-879.
- 50. Woodbury, C. P. The Titration Curve of Weak Polyacids. J. Phys. Chem. 1993, 97, 3623-3630.
- 51. Arnold, R. The Titration of Polymeric Acids. J. Coll. Sci. 1957, 12, 549-556.
- 52. Mandel, M. The Potentiometric Titration of Weak Polyacids. *Eur. Polym. J.* **1970,** *6*, 807-822.
- 53. Sassi, A. P.; Beltran, S.; Hooper, H. H.; Blanch, H. W.; Prausnitz, J.; Siegel, R. A. Monte-Carlo Simulations of Hydrophobic Weak Polyelectrolytes Titration Properties and pH-Induced Structural Transitions for Polymers Containing Weak Electrolytes. *J. Chem. Phys.* **1992**, *97*, 8767-8774.
- 54. Satoh, T.; Sumaru, K.; Takagi, T.; Takai, K.; Kanamori, T. Isomerization of Spirobenzopyrans Bearing Electron-Donating and Electron-Withdrawing Groups in Acidic Aqueous Solutions. *Phys. Chem. Chem. Phys.* **2011**, *13*, 7322-7329.
- 55. Balmond, E. I.; Tautges, B. K.; Faulkner, A. L.; Or, V. W.; Hodur, B. M.; Shaw, J. T.; Louie, A. Y. Comparative Evaluation of Substituent Effect on the Photochromic Properties of Spiropyrans and Spirooxazines. *J. Org. Chem.* **2016**, *81*, 8744-8758.
- 56. Friedle, S.; Thomas, S. W. Controlling Contact Electrification with Photochromic Polymers. *Angew. Chem. Int. Ed.* **2010**, *49*, 7968-7971.
- 57. Hatchard, C. G.; Parker, C. A. A New Sensitive Chemical Actinometer Ii. Potassium Ferrioxalate as a Standard Chemical Actiometer. *Proc. R. Soc. London, Ser. A* **2956**, *235*, 518-536.
- 58. Zhou, J. W.; Li, Y. T.; Tang, Y. W.; Zhao, F. Q.; Song, X. Q.; Li, E. C. Detailed Investigation on a Negative Photochromic Spiropyran. *J. Photochem. Photobiol. A* **1995**, *90*, 117-123.

- 59. Abeyrathna, N.; Liao, Y. Stability of Merocyanine-Type Photoacids in Aqueous Solutions. *J. Phys. Org. Chem.* **2017**, *30*, e3664.
- 60. Wojtyk, J. T. C.; Wasey, A.; Xiao, N. N.; Kazmaier, P. M.; Hoz, S.; Yu, C.; Lemieux, R. P.; Buncel, E. Elucidating the Mechanisms of Acidochromic Spiropyran-Merocyanine Interconversion. *J. Phys. Chem. A* **2007**, *111*, 2511-2516.

# For Table of Contents use only

Title: Tuning the Negative Photochromism of Water Soluble Spiropyran Polymers

Authors: Matthew J. Feeney and Samuel W. Thomas III\*

